XVI IMEKO World Congress
Measurement - Supports Science - Improves Technology - Protects Environment ... and Provides Employment - Now and in the Future
Vienna, AUSTRIA, 2000, September 25-28

TARGET ANALYSIS BY FOCUSING ELLIPSOMETRY

U. Neuschaefer-Rube, W. Holzapfel, and F. Wirth
University of Kassel, Institute for Measurement and Automation
D-34109 Kassel, Germany

Abstract: Reflection ellipsometry is a proven optical measurement method often used to measure film thicknesses. Classical ellipsometers use an unfocused measurement beam, which causes a low lateral resolution in the order of 1 mm. To determine microstructures ellipsometrically (e.g. in the semiconductor industry), an improved lateral resolution in the order of micrometers is essential. We discuss the problems of focusing ellipsometry, occurring when a reflection ellipsometer is used to measure surface characteristics (topography, material). Different measurement setups are analyzed and compared. Simulating calculations show that particularly the measured values of the phase difference Δ are influenced by beam focusing. This leads to errors particularly in the attenuation index k of the surface material.

Keywords: Optical Measurement, Ellipsometry, Beam Focusing

1 INTRODUCTION

Ellipsometers measure the changes in light polarization, when a light beam interacts with the target. In reflection ellipsometers the unfocused measurement beam is reflected at the sample surface. The well-known Fresnel-equations [1] describe the reflection at an uncoated surface. In dependence on the complex refraction index $\underline{n}$ of the surface material and the incidence angle α, two different complex reflection factors $\underline{r}_p$ and $\underline{r}_s$ exist, corresponding to the light portions polarized parallel (p) or perpendicular (s) to the incidence plane. Reflection ellipsometers determine the ratio $\underline{r}_p/\underline{r}_s$ characterized by the ellipsometric parameters, i. e. polarization-dependent loss angle Ψ and phase difference Δ. To measure Ψ and Δ, the sample is arranged in a PSA (Polarizer-Sample-Analyzer)-ellipsometric configuration or in a PCSA (Polarizer-Compensator-Sample-Analyzer)-ellipsometer. Light with a well-defined polarization state irradiates on the sample. To analyze the polarization state of the reflected light and to gain the ellipsometric parameters several measurement procedures [2] (e.g. Null-Ellipsometry, Rotating-Analyzer Ellipsometry, Modulated Ellipsometry) are applicable.

If the light is reflected at a coated surface, multiple reflections occur. The polarization state of the reflected light beam results from the interference of the light portions reflected at the interfaces between the layers [2]. In this case, the ellipsometric parameters Ψ and Δ depend on the refraction indices of the layer materials and the film thicknesses. This dependence is often used to measure film thicknesses ellipsometrically with nm resolution (e.g. [3]).

Today‘s ellipsometers use unfocused measurement beams. Therefore their lateral resolution is limited to the order of 1 mm. An important application field is film thickness measurement in the semiconductor industry. An improvement of the lateral resolution to the order of 1 μm using focused beams would open new applications for ellipsometry. Target microstructures could be measured e.g. to check the etch process in the production of microchips.

2 ELLIPSOMETERS WITH FOCUSED BEAM

2.1 Modeling of a focused beam

When the measurement beam is focused, a convergent beam is irradiating on the target. This beam can be modeled as a cone of elementary beams which differ in polarization and incidence plane (e.g. [4]). This effect is called polarization aberration. Integrating the elementary beam intensities yields the resulting intensity, detected behind the PSA- or PCSA-ellipsometer arrangement. In [4] the errors caused by the beam convergence are analyzed theoretically. Unfortunately some simplifying assumptions are made: the Gaussian intensity distribution of the measurement beam and the influence of the main-axis orientation φ are neglected and the calculations are made for a particular measurement setup. We conclude that errors caused by the convergent beam can only be calculated theoretically using iterative methods. The disadvantage of this procedure is, there can‘t be any theoretical formulas derived to compensate the convergence effect. A new approach to ellipsometric beam configuration is essential. That is because the amount of the convergence errors is influenced by the measurement setup.

2.2 Ellipsometer with internal focusing elements

To measure with focused measurement beam a focusing lens L_1 and a collimating lens L_2 must be added to the ellipsometer. Fig. 1a shows a feasible PSA-reflection-ellipsometer configuration with focused measurement beam. In Fig. 1a the lenses are placed within the PSA-arrangement. Therefore it is possible to use lenses with short focal lengths. This facilitates a high local resolution but increases the polarization aberration.

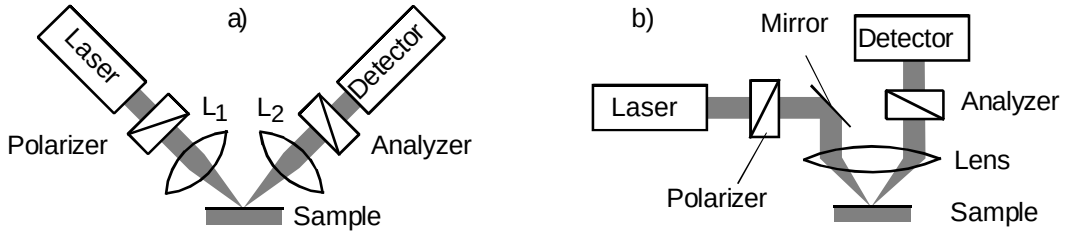

Figure 1. PSA-reflection-ellipsometer with internal focusing elements.
a) basic configuration, b) configuration with a single lens.

The device under test in the ellipsometer consists of the series connection L_1-Sample-L_2. Using the Jones matrix formalism, the electric field vector $\mathbf{E}_{Det}$, measured by the detector is:

$$\mathbf{E}_{Det} = \mathbf{A} \cdot \mathbf{L}_2 \cdot \mathbf{R}(-\varphi) \cdot \begin{bmatrix} \tan\Psi \cdot e^{i\Delta} & 0 \\ 0 & 1 \end{bmatrix} \cdot \mathbf{R}(\varphi) \cdot \mathbf{L}_1 \cdot \mathbf{P} \cdot \mathbf{E}_{Laser} \qquad (1)$$

(**R:** Rotation matrix, **A**, $\mathbf{L}_2$, $\mathbf{L}_1$, **P**: Jones matrices of analyzer, collimation lens, focusing lens, polarizer, $\mathbf{E}_{Laser}$: electric field vector of the incident laser beam). Birefringence of the lenses causes errors in the measured ellipsometric parameters. Therefore, lenses free of mechanical stresses are necessary.

In this configuration, it is conceivable that the beam focusing and collimating is performed by the same lens (Fig. 1b). In this case, optics with very short focal length (1 mm - 2 mm) can be used. Unfortunately, only a portion of the lens aperture can be utilized for the incident beam. This reduces the achievable lateral resolution.

The polarization abberation can be neglected if the diameter of the input beam in the lens aperture is small compared to the focal length of the lens. In this case the effect of the lens on the beam polarization in the configuration shown in Fig. 1b can be reduced to coordinate rotations occurring at the principal plane of the lens when the beam is focused and collimated [5, 6]. Using a lens with neglectable birefringence (objective for polarization microscopes) and a non-polarizing mirror, the detected electric field vector follows from the equation:

$$\mathbf{E}_{Det} = \mathbf{A} \cdot \mathbf{R}(\vartheta_o) \cdot \mathbf{R}(-\varphi) \cdot \begin{bmatrix} \tan\Psi \cdot e^{i\Delta} & 0 \\ 0 & 1 \end{bmatrix} \cdot \mathbf{R}(\varphi) \cdot \mathbf{R}(\vartheta_i) \cdot \mathbf{P} \cdot \mathbf{E}_{Laser} \qquad (2)$$

The coordinate rotations depend on the azimuths ϑ_i and ϑ_o of the input and output beam in the lens aperture. Therefore, the coordinate rotation, occurring when the reflected beam is collimated by the lens, depends on the slope angle of the sample surface. We used this configuration to determine the surface topography and material simultaneously [5, 6]. The surface topography is concluded from the measured ellipsometric parameters ϑ_o and φ. When the surface topography is determined, the refraction index $\underline{n}$ of the surface material follows from the measured parameters Δ and Ψ. To measure the four wanted ellipsometric parameters a new eight-zone measurement algorithm was developed.

2.3 Ellipsometer with external focusing elements

If the lenses are placed in front of the polarizer and behind the analyzer (Fig. 2), the detected electric field intensity $\mathbf{E}_{Det}$ is

$$\mathbf{E}_{Det} = \mathbf{A} \cdot \mathbf{R}(-\varphi) \cdot \begin{bmatrix} \tan\Psi \cdot e^{i\Delta} & 0 \\ 0 & 1 \end{bmatrix} \cdot \mathbf{R}(\varphi) \cdot \mathbf{P} \cdot \mathbf{E}_{Laser} \qquad (3)$$

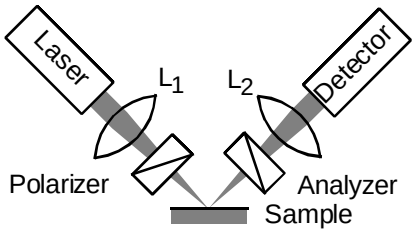

Figure 2. PSA-reflection ellipsometer with external focusing elements.

The elementary beams are passing polarizer and analyzer under different angles. Therefore, the effective polarizer and analyzer azimuths of the elementary beams are different. Since a comparatively long focal length of the lenses is necessary, a beam with small divergence is hitting the sample. This causes a small polarization aberration, but limits the achievable lateral resolution. Optical anisotropies of the lenses do not influence the ellipsometric result.

The direction of the reflected beam passing the analyzer depends on the slope of the sample topography. Therefore an analyzer with great aperture is necessary. To avoid a rotation of the analyzer while the ellipsometric measurement, we developed a new ellipsometric algorithm based on intensity measurements at three different polarizer azimuths (zones). Because of the small beam divergence the polarization aberration was neglected for the moment. Using the intensities I_0, I_{90}, I_{135}, measured at the polarizer azimuths 0°, 90°, 135°, the ellipsometric parameters Δ and Ψ are determined by the equations:

$$\Psi = \mathrm{ArcTan}\left(\frac{(I_0 + I_{90} + (I_0 - I_{90}) \cdot \cos(2\varphi) + (I_0 - 2I_{135} + I_{90}) \cdot \sin(2\varphi)) \cdot \tan(a + \varphi)}{\sqrt{-2I_{135} \cdot (I_{135} - I_{90}) + 2I_0 \cdot (I_{135} + I_{90}) - 2(I_0 - I_{135}) \cdot (I_{135} - I_{90}) \cdot \cos(4\varphi)}} \right) \qquad (4)$$

$$\Delta = \mathrm{ArcCos}\left(\frac{(I_0 - 2I_{135} + I_{90}) \cdot \cos(2\varphi) + (-I_0 + I_{90}) \cdot \sin(2\varphi)}{\sqrt{-2I_{135} \cdot (I_{135} - I_{90}) + 2I_0 \cdot (I_{135} + I_{90}) - 2(I_0 - I_{135}) \cdot (I_{135} - I_{90}) \cdot \cos(4\varphi)}} \right) \qquad (5)$$

In the following, we are calling this algorithm “three-zone algorithm“. To calculate Ψ and Δ using Eq. (1, 2), the main-axis orientation φ must be known. Furthermore, the analyzer azimuth a is needed to calculate Ψ.

The main-axis orientation φ depends on the surface topography. In contrast to the arrangement described in chapter 2.2, the topography cannot be concluded from ellipsometric data of the three-zone algorithm. Therefore, we have to measure the topography using a different measurement principle (e.g. triangulation, autofocus topometry).

In dependence on the surface topography, the reflected beam passes the analyzer at an angle and the effective analyzer azimuth is changed. Therefore, the analyzer azimuth used in Eq. (4) depends on the surface topography.

To check the new algorithm we first carried out successful tests using an unfocused beam. We conclude from our measurement results that the refraction index of different metals (gold, steel) was measured with an accuracy of approx. ±0.02. The real part n of a dielectric material (glass) was measured with an accuracy of approx. ±0.005. However, the imaginary part k was measured only with an accuracy in the order of 0.1. The reason for this characteristic is, that the algorithm (see Eq. (5)) determines the value $\cos(\Delta)$. This leads to significant measurement errors in the case of dielectric materials because their phase difference Δ is 180°.

3 SIMULATION OF FOCUSING ELLIPSOMETRY

3.1 Simulation procedure

We made simulating calculations to investigate the influence of the beam focusing on the measured ellipsometric parameters. The eight-zone ([5], [6]) and the three-zone (Eq. 4, 5) measurement algorithm was investigated. The measurement beam with a gaussian intensity profile was splitted into approx. 500 elementary beams. Taking the individual incidence angle, incidence plane and effective

polarizer/analyzer azimuths into account, the transmitted intensity of each elementary beam was calculated. This calculation was made for every zone. Finally, we calculated the sum of the elementary beam intensities in the zones and put the results into the formulas of the measurement algorithms (e.g. Eq. (4,5)) in order to calculate the resulting ellipsometric parameters (marked with the index "f").

In the calculations we used data of realistic focusing optics: The simulations of the eight-zone measurement algorithm (ellipsometer with a single focusing lens according to Fig. 1b) were made assuming a 100x microscope objective (NA = 0.95). The simulations of the three-zone algorithm (ellipsometer according to Fig. 2) were made assuming a lens with a focal length f = 100 mm with diameter d_{lens} = 50 mm.

In all calculations we choosed a mean incidence angle α_{mean} = 45°. In this case we obtain a great sensitivity of the refraction index determination and avoid the problematic measurement of small Ψ-values occurring at incidence angles near the Brewster angle, caused by the limited extinction ratios of polarizer and analyzer.

The resulting ellipsometric parameters were calculated in dependence on the amount of beam focusing, described by the waist diameter d of the focused beam (= width of the measurement spot on the surface). The light wavelength was set to λ = 442 nm. We assumed that the diameter of the unfocused beam has to fit at least 2.5 times into the lens aperture. In this case in both algorithms the minimum waist diameter is approx. 2.8 μm.

3.2 Simulated measurement of a glass surface

The first simulation was made assuming a plane glass surface (n = 1.5, k = 0) to be measured.

An important result of the simulation of the eight-zone algorithm is, that the measured parameters φ and ϑ_0 are not affected by beam focusing. Therefore, the ellipsometric measurement of the topography can be performed without errors caused by beam focusing.

In both algorithms, the parameters Ψ_f and Δ_f depend on the beam focusing (Fig. 3).

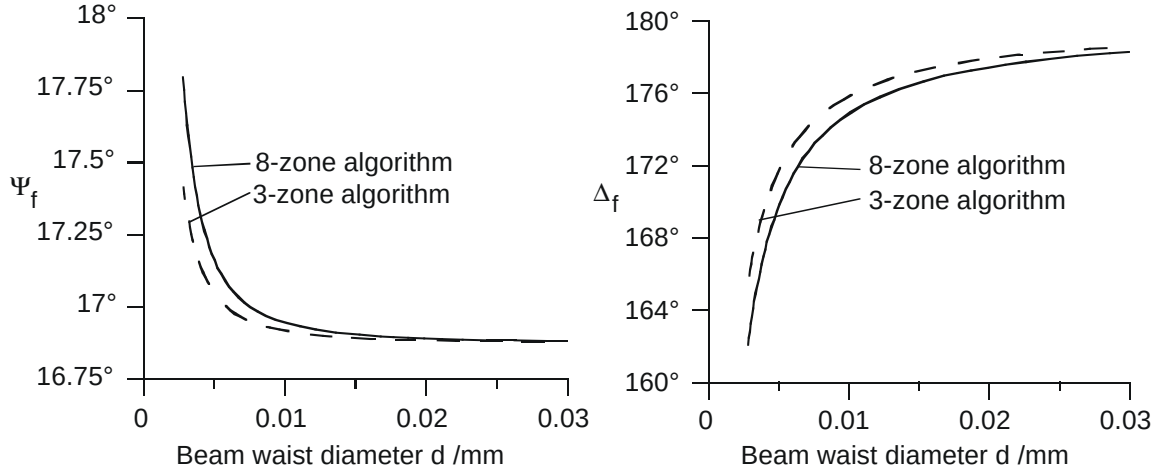

Figure 3. Calculated ellipsometric parameters Ψ_f and Δ_f in dependence on the diameter d of the beam waist (light wavelength λ = 442 nm, mean incidence angle α_{mean} = 45°, device under test: plane glass surface (n = 1.5, k = 0)).

The errors increase with decreasing diameter of the beam waist. While the changes in the polarization-dependent loss angle Ψ are smaller than 1°, the values of the phase difference Δ decreases by more than 15°, if the beam is focused maximally. The deviation of Ψ_f from the correct value 16.87° is very small if the beam is only slightly focused (d 30 μm). Unfortunately, in this case the measured Δ-values differ significantly from the correct value of 180°. The results of the eight-zone algorithm are slightly more influenced by beam focusing.

An important intention of the ellipsometric measurement of the parameters Ψ and Δ is to identify the surface material by it's complex refraction index. The complex refraction index $\underline{n}$ = n - jk follows from the measured ellipsometric parameters Δ, Ψ and the incidence angle α. Modifying the formula in [1], we determined the following equations to calculate the real part n and imaginary part k of the refraction index $\underline{n}$:

$$n = \frac{\sqrt{A + \sqrt{A^2 + B^2}}}{\sqrt{2}}, \quad k = \frac{B}{2 \cdot n} \qquad (6\ a,b)$$

with the abbreviations

$$A = \sin^2\alpha \cdot \left(1 + \tan^2\alpha \cdot \frac{\cos^2(2\Psi) - \sin^2\Delta \cdot \sin^2(2\Psi)}{(1+\sin(2\Psi)\cdot\cos\Delta)^2}\right), \quad B = \frac{\sin^2\alpha \cdot \tan^2\alpha \cdot \sin(4\Psi)\cdot\sin\Delta}{(1+\sin(2\Psi)\cdot\cos\Delta)^2} \qquad (7a,b)$$

Fig. 4 shows the dependence of the real part n and the imaginary part k of the complex refraction index $\underline{n}$ on beam focusing using the data of Fig. 3.

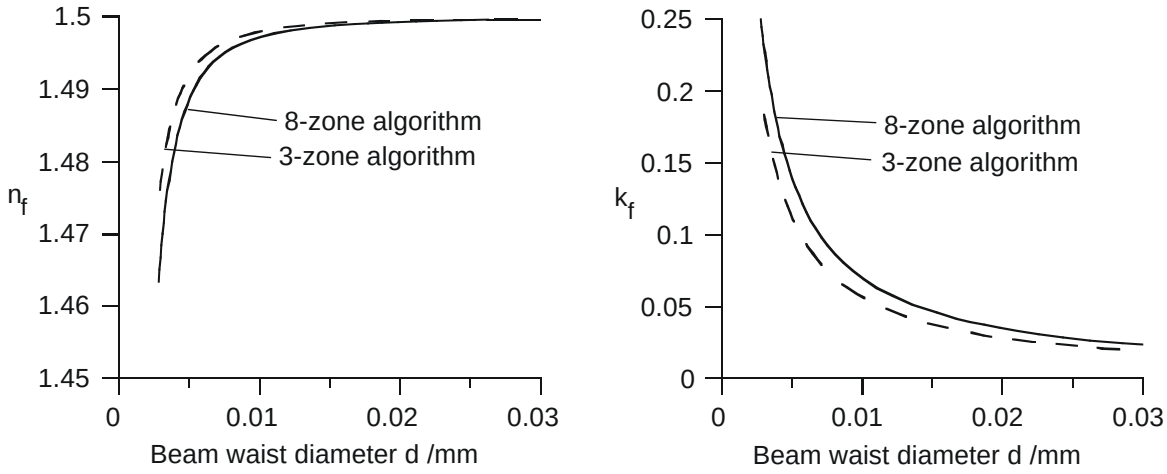

Figure 4. Calculated real part n_f and imaginary part k_f of the refraction index in dependence on the beam waist diameter d (light wavelength λ = 442 nm, mean incidence angle α_{mean} = 45°, device under test: plane glass surface (n = 1.5, k = 0)).

The real part n decreases by max. 0.035 if the beam is focused maximally. The error caused by beam focusing can be neglected if d 30 μm. The imaginary part k (attenuation index) increases by max. 0.25. These changes are mainly caused by the errors of the phase difference Δ. These errors can only be neglected if the beam waist diameter d is much greater than 30 μm.

3.3 Simulated measurement of a gold surface

Fig. 5 shows the simulated dependence of the beam focusing on the measured refraction index, when a plane gold surface is measured. We used the refraction index $\underline{n}$ = 1.316 - j1.749 determined by own ellipsometric measurements with unfocused beam.

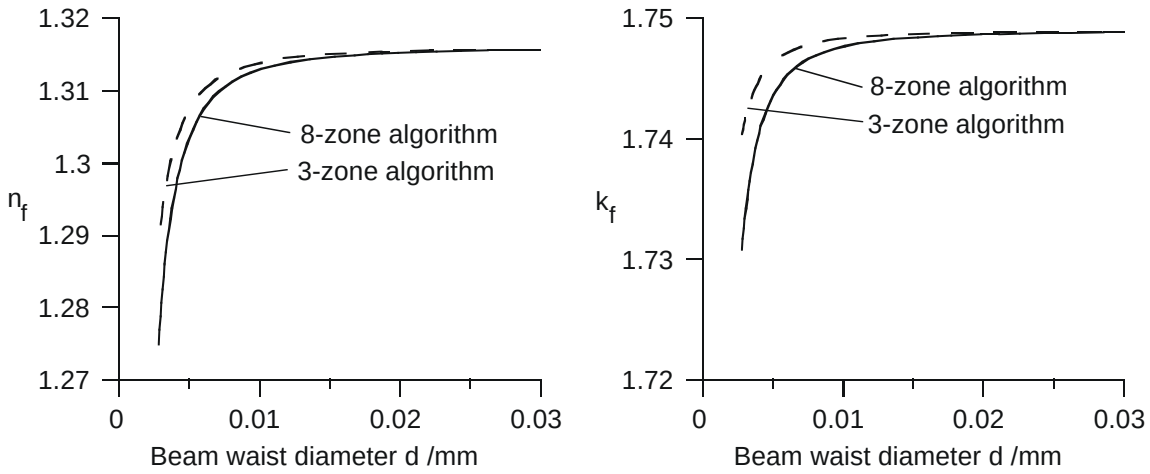

Figure 5. Calculated real part n_f and imaginary part k_f of the refraction index in dependence on the beam waist diameter d (light wavelength λ = 442 nm, mean incidence angle α_{mean} = 45°, device under test: plane gold surface (n = 1.316, k = 1.749)).

The maximum errors in n and k are in the order of 0.035 and 0.02, respectively. In contrast to the result assuming a glass surface, the error of the imaginary part k is smaller than the error of the real

part n. Moreover, the imaginary part k decreases when the measurement beam is focused. The errors in n and k can be neglected if the beam is only slightly focused (d 30 μm).

3.4 Errors in dependence on the surface material

Fig. 6 shows the errors $e_n = n_f - n$ and $e_k = k_f - k$ in dependence on the complex refraction index of surface material. In the calculation we assumed that the three-zone algorithm is used and that the measurement beam is focused maximally (d = 2.8 μm).

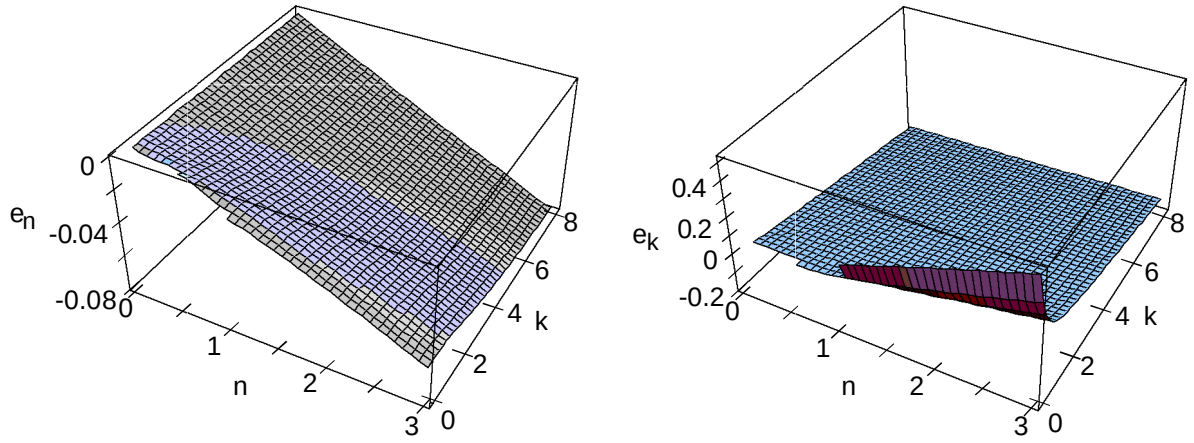

Figure 6. Errors $e_n = n_f - n$ and $e_k = k_f - k$ caused by beam focusing in dependence on the complex refraction index $\underline{n} = n - jk$ of the surface material (3-zone algorithm, beam waist diameter d = 2.8 μm, light wavelength λ = 442 nm).

The error e_n of the real part n increases nearly proportional to the value n. $|e_n|$ is always smaller than 0.08. There is only a small influence of k.

The greatest error e_k of the imaginary part k occurs if the surface material is dielectric (k = 0). The calculation yields positive and negative e_k-values. The maximum error e_k is approx. 0.4.

4 CONCLUSIONS AND PROSPECTS

Focusing the measurement beam causes changes in the measured ellipsometric parameters Δ and Ψ. While the polarization-dependent loss angle Ψ is only slightly affected by beam focusing, the phase difference Δ changes in the order of degrees when a material with a small attenuation index k is measured. The calculation of the complex refraction index using the ellipsometric parameters yields small errors in the real part n. The imaginary part k is considerably affected by beam focusing, if k is small. Errors up to 0.4 are possible. Therefore the measurement of dielectric materials (k = 0) is critical. These results are nearly unaffected by the measurement algorithm.

In further investigations we will simulate the measurement of film systems with a focused measurement beam. To compensate the beam-focusing effect, we will investigate correction procedures.

REFERENCES

[1] Born, Wolf, *Principles of Optics*, Pergamon Press, Oxford, 1987.
[2] R. M. A. Azzam, N. M. Bashara, *Ellipsometry and Polarized Light*, N. Holland, Amsterdam, 1977.
[3] R. M. A. Azzam (Ed.), *Selected Papers on Ellipsometry*, SPIE Milestone Series, Vol. MS 27, SPIE Optical Engineering Press, 1991.
[4] D. O. Barsukov, G. M. Gusakov, A. A. Komarskii: Precision ellipsometry on a focused light beam. Part 1, *Optics and Spectroscopy* **64**, (1988) 782-785.
[5] W. Holzapfel, U. Neuschaefer-Rube, J. Doberitzsch, Measurement of Surface Topography and Material by Micro-Ellipsometry, in: *Proceedings of IMEKO XV World Congress* (Osaka, Japan, June 13-18, 1999) Vol. IX, 63-69.
[6] W. Holzapfel, U. Neuschaefer-Rube, J. Doberitzsch, F. Wirth, Präzise Strukturmeßtechnik mit lasergestützter Mikroellipsometrie, *Technisches Messen* **66** (11) (1999) 455-462.

AUTHORS: Ulrich NEUSCHAEFER-RUBE, Wolfgang HOLZAPFEL and F. WIRTH, University of Kassel, Institute for Measurement and Automation, D-34109 Kassel, Germany, Phone: ++49 561 8042756, Fax: ++49 561 8042847, E-mail: unr@imat.maschinenbau.uni-kassel.de